ELSEVIER

April 2001

Materials Letters 48 (2001) 184–187

MATERIALS LETTERS

www.elsevier.com/locate/matlet

Thick amorphous ferromagnetic coatings via thermal spraying of spark-eroded powder

F.T. Parker [a,*], F.E. Spada [a], A.E. Berkowitz [a], K.S. Vecchio [b], E.J. Lavernia [c], R. Rodriguez [c]

[a] *Center for Magnetic Recording Research, University of California—San Diego, La Jolla, CA 92093-0401, USA*
[b] *Department of Mechanical and Aerospace Engineering, University of California—San Diego, La Jolla, CA 92093-0411, USA*
[c] *Department of Mechanical and Aerospace Engineering, University of California—Irvine, Irvine, CA 92697-2575, USA*

Received 11 September 2000; accepted 23 October 2000

Abstract

300-μm thick amorphous ferromagnetic coatings were prepared by thermally spraying amorphous $Fe_{75}Si_{15}B_{10}$ powder. The amorphous feedstock powder for the thermal spraying was made by the spark-erosion method. The Mössbauer, X-ray diffraction, chemical, and magnetic properties of the coatings were very similar to those of the spark-eroded powder. Consolidated magnetic amorphous materials have long been a technological goal, and are expected to provide substantial electrical energy savings. © 2001 Elsevier Science B.V. All rights reserved.

PACS: 75.50.Kj; 81.15.Rs; 82.80.Ej
Keywords: Amorphous magnetic materials; Thermal spray coating; Mössbauer effect analysis

Electrical transformer and motor losses amount to about 1% of the electrical energy produced in the United States [1]. Thus, a replacement has been sought for the current transformer laminas, 300-um-thick crystalline Fe–Si. Amorphous ferromagnetic materials can have much lower hysteresis losses. However, one generally needs very rapid quench rates from a gaseous or molten state to obtain amorphous phases. This necessitates very thin layers, such as melt-spun Metglass™, which has proven difficult to manipulate. Some particular composition alloys have large differences between glass and crystallization temperatures [1,2], and thus can be shaped at elevated temperature.

Amorphous ferromagnetic particles can be produced by spark erosion in a dielectric liquid, which provides the extremely rapid cooling needed to prevent crystallization [3,4]. As a means of consolidating amorphous $Fe_{75}Si_{15}B_{10}$ particles into a bulk form, we have used the technique of high velocity oxy-fuel (HVOF) thermal spraying. This technique tends to produce coatings with low porosity and high cohesive strength [5]. The HVOF technique provides

* Corresponding author. Tel.: +1-858-534-6214; fax: +1-858-534-2720.
E-mail address: fspada@ucsd.edu (F.T. Parker).

PII: S0167-577X(00)00300-1

relatively cool gas stream temperatures and high substrate impact velocities compared to other spraying techniques, which should provide high quality coatings with relatively small amounts of crystallization and oxidation. The sprayed coating is found to be primarily composed of amorphous Fe–Si–B alloy with magnetic properties and Mössbauer effect properties similar to the pre-sprayed particles, even though some of the particles exceeded both their crystallization and melting temperatures during the spraying process.

Amorphous $Fe_{75}Si_{15}B_{10}$ particles were prepared by spark erosion in dodecane, with preparation conditions generally similar to those reported earlier [3,4]. There was no size selection of particles, which ranged from about 0.5 to 40 um. The particles were thermally sprayed with a Sulzer Metco DJ5000 HVOF unit onto mild steel substrates 3 mm in thickness. The main constituents of this facility are as follows: (1) a DJC control unit, (2) a 0-MP hopper feeder, (3) a "Parker" X-Y automated traverse unit, (4) "In-Flight" diagnostic equipment and (5) the Diamond Jet spray gun. The DJC control unit monitors and controls the gas flow into the gun and allows the proper stoichiometric ratios to be set for optimum spray performance which were the following for the $Fe_{75}Si_{15}B_{10}$ coating deposition: 100 psi for propylene, 150 psi for oxygen, and 100 psi for air. The 9-MP powder feeder is a fluidized bed powder feed unit that allows proper control of the powder flow into the gun and was set to 150 psi with nitrogen as the carrier gas. To produce uniform coatings, a "Parker" automated X-Y system was installed on the HVOF system. With the "In-Flight" diagnostic equipment, accurate average particle temperatures can be measured as well as trajectory and particle flow characteristics. The Diamond Jet spray gun is a hybrid water-cooled gun that allows easy transitions between the possible fuel gases, hydrogen and propylene. This gun produces a hypersonic, low temperature flame with gas velocities of 1830 m/s and temperatures around 2700 K.

The 300-μm coating was cut from the mild steel plate, and both sides were ground to yield a final coating thickness of 40 μm, which is appropriate for ^{57}Fe Mössbauer spectroscopy. Characterization techniques included X-ray diffractometry, scanning electron microscopy (SEM), and magnetization measurements with a vibrating sample magnetometer. All measurements were performed at room temperature. The Mössbauer source was ^{57}Co in Rh. The velocity calibration and isomer shift reference were obtained with an Fe foil. The part of each Mössbauer spectrum representing amorphous material was least-squares fit to a distribution ($P(H)$) in hyperfine field (H). These subspectra were constrained to have a common isomer shift (IS). Other subspectra representing impurity phases in the sprayed coating had independent fitting variables. Some of the hyperfine interaction parameters obtained from these subspectra were fixed in the fits of the spark-eroded particle spectrum.

Mössbauer data and fits are shown in Fig. 1a and b. The spectra for the powder and coating appear similar, with predominantly broad lines characteristic of the many local environments in magnetically split amorphous materials. Some additional sharper lines are visible in the spectrum for the coating, representing crystalline phases. The hyperfine field distributions are compared in Fig. 1c. A slight shift to higher values of H is evident for the envelope describing the $P(H)$ curve for the coating. A summary of the Mössbauer and magnetization data is given in Table 1. The primary crystalline impurities in the coating are seen to be α-Fe ($\sim$ 4 met. at.%) and a paramagnetic quadrupole-split phase ($\sim$ 2 met. at.% Fe) with an IS characteristic of Fe^{2+}. Additionally, about 1 met. at.% Fe is present as magnetite. Another 1 met. at.% Fe has a value of H which is just below that of Fe metal, and might represent bcc $Fe_{(1-x)}Si_x$ ($x \sim 0$) alloy [6]. From the slightly irregular shape of the $P(H)$ curve for the amorphous material in the coating, there is also likely a few percent of Fe in other magnetically split crystalline Fe–Si–B phases. For the powder, the only impurity is 2 met. at.% Fe in a paramagnetic material with an IS close to those typically found for Fe^{3+}.

Magnetization data (Table 1) show a slight increase in the saturation magnetization of the coating compared to that of the powder. X-ray diffraction patterns (not shown) exhibit peaks with broad maxima for both powder and coated material. The powder also shows a few minor, narrow crystalline peaks, which were not indexed. The dominant impurity for the coated material can be indexed as α-Fe in agreement with the Mössbauer results. SEM images of the

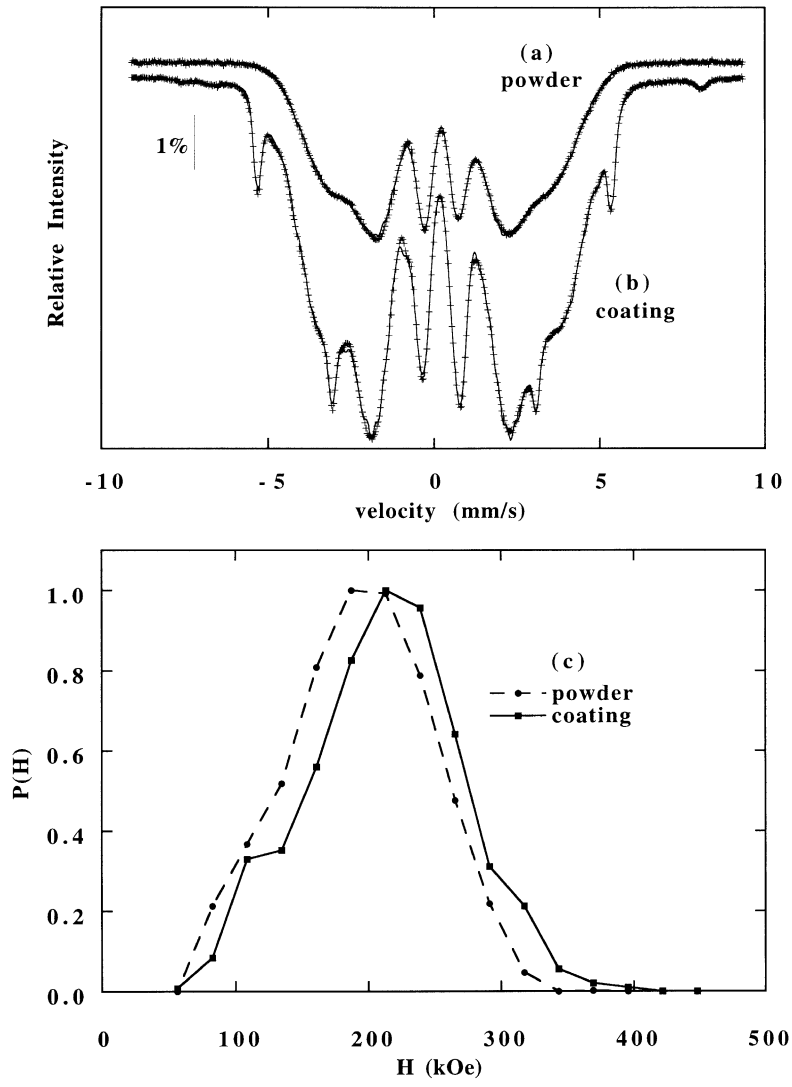

Fig. 1. Mössbauer data (pluses) and least-squares fits (lines) for $Fe_{75}Si_{15}B_{10}$ powder (a) and HVOF-sprayed coating (b). The hyperfine field distributions for the amorphous phase in each spectrum are compared in (c), with each $P(H)$ distribution normalized to the same maximum value.

spray-deposited sample (not shown) exhibited porosity $\sim$ 18%, which is high compared to typical values (e.g., 2% porosity measured by fluid immersion techniques for spray-deposited Ni particles) [5]. Part of the difference might be due to voids found in the spark-eroded particles [7].

The coating exhibits two primary differences relative to the powder: the presence of a small amount of α-Fe and a slight increase in $\langle H \rangle$, the average magnetic hyperfine field of the amorphous material. The most likely cause for the formation of Fe metal is partial oxidation of the coating. B and Si are far more reactive with O_2 than Fe [8], and thus would be expected to preferentially oxidize, leaving α-Fe and lesser amounts of Fe oxide. Crystallization of the particles results in iron silicide and iron boride compounds, and not elemental Fe [9]. The small amount of α-Fe in the coating suggests minimal oxidation,

Table 1
Mössbauer effect and magnetization data from spark-eroded powders and coating sprayed by the HVOF technique

	Powder	Coating
a-$Fe_{75}Si_{15}B_{10}$		
⟨H⟩ (kOe)	193	212
sd (kOe)	53	58
⟨IS⟩ (mm/s)	0.20(1)	0.20(1)
Fractions (%)		
a-$Fe_{75}Si_{15}B_{10}$	98.0	92.0
Fe metal	0.4(1)	4.2(2)
metalloid	–	1.0(1)
magnetite A	0.0(1)	0.3(1)
magnetite B	0.0(1)	0.6(1)
paramagnetic phase	1.6(1)	1.9(1)
Magnetization (emu/g)	132	139
Coercivity (Oe)	39	25

For the amorphous $Fe_{75}Si_{15}B_{10}$ (a-$Fe_{75}Si_{15}B_{10}$) entry, only the magnetically split subspectra included in the $P(H)$ data are included in the calculations. "sd" refers to the standard deviation in H. For the powder calculations, some hyperfine interaction parameters were fixed as found for the coating spectrum. "Fractions" denotes the metal at.% Fe in each of the phases. Statistical error in the last digit is shown in parentheses.

which could be decreased in future preparations by increasing the fuel/oxygen ratio in the HVOF process.

There are several possible mechanisms for the increase in $\langle H \rangle$ for the coating. Smaller particles get hotter in the HVOF process than larger particles [10], and thus are far more likely to oxidize. This will cause an increase in $\langle H \rangle$, since smaller particles have lower values of $\langle H \rangle$ [3,4]. However, only about 5% of the material oxidized. If one assumes that only the smallest particles are oxidized, the resultant shift in $\langle H \rangle$ can be calculated to be only about 1 kOe, far less than the observed 19 kOe. Preferential internal oxidation of B and Si would also increase $\langle H \rangle$, but is unlikely since larger particles would remain solid and only surface oxidation is expected to occur, as shown by the formation of B_2O_3 on the surface of crystalline Fe_2B [11].

Another possible reason for the increase in $\langle H \rangle$ is melting and refreezing of the smaller particles and grain growth occurring on the substrate [5]. Since $\langle H \rangle$ increases, the freezing process is apparently sufficiently fast to maintain the amorphous nature, but not as fast as it occurs during spark erosion [3,4]. Particles which are heated above the normal crystallization temperature but not to the melting point apparently do not have time to crystallize before cooling. Annealing particles with this composition at temperatures somewhat below crystallization increases the magnetization (and thus $\langle H \rangle$) by about 3% [7], far less than the 10% increase in $\langle H \rangle$ observed. A similar 3% increase in $\langle H \rangle$ was found [12] just below the crystallization temperature in amorphous $Fe_{82}B_{12}Si_6$.

Optimization of this promising method of obtaining thick amorphous magnetic coatings would include varying the feedstock particle size distribution and HVOF processing conditions.

Acknowledgements

EJL and RR gratefully acknowledge financial support provided by the Office of Naval Research under grants N00014-94-1-0017, N00014-97-1-0844 and N00014-98-1-0569. We thank M.F. Hansen for experimental assistance.

References

[1] T.D. Shen, R.B. Schwarz, Appl. Phys. Lett. 75 (1999) 49.
[2] A. Inoue, Mater. Sci. Eng., A 226–228 (1997) 357.
[3] A.E. Berkowitz, J.L. Walter, K.F. Wall, Phys. Rev. Lett. 46 (1981) 1484.
[4] A.E. Berkowitz, J.L. Walter, J. Mater. Res. 2 (1987) 277.
[5] M.L. Lau, H.G. Jiang, W. Nuchter, E.J. Lavernia, Phys. Status Solidi A 166 (1998) 257.
[6] M.B. Stearns, Phys. Rev. 129 (1963) 1136.
[7] A.E. Berkowitz, J.L. Walter, Mater. Sci. Eng. 55 (1982) 275.
[8] Handbook of Chemistry and Physics, Chemical Rubber Publ., Cleveland, OH, 1960.
[9] J.L. Walter, A.E. Berkowitz, E.F. Koch, Mater. Sci. Eng. 60 (1983) 31.
[10] M.L. Lau, V.V. Gupta, E.J. Lavernia, Nanostruct. Mater. 10 (1998) 715.
[11] M. Carbucicchio, R. Reverberi, G. Palobarini, G. Sambogna, Hyperfine Interact. 46 (1989) 473.
[12] H.N. Ok, A.H. Morrish, Phys. Rev. B 22 (1980) 3471.